Disorder raises the critical temperature of a cuprate superconductor

Maxime Leroux[a,1,2], Vivek Mishra[a,3], Jacob P. C. Ruff[b], Helmut Claus[a], Matthew P. Smylie[a,4], Christine Opagiste[c], Pierre Rodière[c], Asghar Kayani[d], G. D. Gu[e], John M. Tranquada[e], Wai-Kwong Kwok[a], Zahirul Islam[f], and Ulrich Welp[a,1]

[a]Materials Science Division, Argonne National Laboratory, Lemont, IL 60439; [b]Cornell High Energy Synchrotron Source, Cornell University, Ithaca, NY 14853; [c]Institut Néel, CNRS, Université Grenoble Alpes, 38042 Grenoble, France; [d]Department of Physics, Western Michigan University, Kalamazoo, MI 49008; [e]Condensed Matter Physics and Materials Science Department, Brookhaven National Laboratory, Upton, NY 11973; and [f]Advanced Photon Source, Argonne National Laboratory, Lemont, IL 60439

Edited by J. C. Séamus Davis, Cornell University, Ithaca, NY, and approved April 5, 2019 (received for review October 4, 2018)

With the discovery of charge-density waves (CDWs) in most members of the cuprate high-temperature superconductors, the interplay between superconductivity and CDWs has become a key point in the debate on the origin of high-temperature superconductivity. Some experiments in cuprates point toward a CDW state competing with superconductivity, but others raise the possibility of a CDW-superconductivity intertwined order or more elusive pair-density waves (PDWs). Here, we have used proton irradiation to induce disorder in crystals of $La_{1.875}Ba_{0.125}CuO_4$ and observed a striking 50% increase of T_c, accompanied by a suppression of the CDWs. This is in sharp contrast with the behavior expected of a d-wave superconductor, for which both magnetic and nonmagnetic defects should suppress T_c. Our results thus make an unambiguous case for the strong detrimental effect of the CDW on bulk superconductivity in $La_{1.875}Ba_{0.125}CuO_4$. Using tunnel diode oscillator (TDO) measurements, we find indications for potential dynamic layer decoupling in a PDW phase. Our results establish irradiation-induced disorder as a particularly relevant tuning parameter for the many families of superconductors with coexisting density waves, which we demonstrate on superconductors such as the dichalcogenides and $Lu_5Ir_4Si_{10}$.

disorder | superconductivity | charge order | pair-density wave | cuprates

Charge-density waves (CDWs) are real-space periodic oscillations of the crystal electronic density accompanied by a lattice distortion. In their simplest form, CDWs can be described as a Bardeen–Cooper–Schrieffer condensate of electron-hole pairs that breaks the translational symmetry (1). CDWs in cuprate superconductors were first observed in lanthanum-based compounds (2–4), such as $La_{2-x}Ba_xCuO_4$ (LBCO) with $x \sim 1/8$ hole-doping (2, 4–12). In these La-based cuprates, spin correlations were also found to synchronize with the CDW modulation to form static "stripes" (2) of interlocked CDWs and spin-density waves (SDWs) at a certain temperature below the ordering temperature of the CDWs (Fig. 1).

More recently, CDWs were shown to be a nearly universal characteristic in cuprates: A CDW was observed in hole-doped $YBa_2Cu_3O_{7-\delta}$ (YBCO) (13–19), as well as several other hole-doped cuprates (20, 21), and it was also found in electron-doped $Nd_{2-x}Ce_xCuO_4$ (22). These CDWs seemed at first notably different from the stripes in La-based cuprates, as they were not accompanied by an SDW. But recent studies suggest that the 3D CDWs induced by magnetic fields in YBCO might have connections with LBCO in terms of a pair-density wave (PDW) state (23, 24).

The role of these density waves in the bigger picture of high-temperature superconductivity is subject to intense and active research (25). To first order, CDWs and superconductivity compete for the same electronic density of states near the Fermi level, as was observed in several s-wave CDW superconductors, such as 2H-TaS/Se_2 (26) and $Lu_5Ir_4Si_{10}$ (27–29). Indeed, in cuprate superconductors, the current experimental evidence seems to point toward a scenario where the CDW state is in competition with bulk superconductivity. The superconducting T_c exhibits a plateau (30, 31) or a deep minimum (6, 32) in the range of doping where the CDW occurs. X-ray studies in YBCO also found that the CDW phase is suppressed when entering the superconducting phase (16). Conversely, the CDW was found to be enhanced when superconductivity was suppressed by a magnetic field (17–19, 33), and the superconducting critical temperature could be restored when the CDW was suppressed under pressure (34). Despite this range of results in favor of competition, a definitive consensus has not yet been reached, as the tuning parameters mentioned above may have nontrivial beneficial or detrimental effects on both superconductivity and CDWs, considering the complex mix of charge, spin, and electronic orders involved.

Moreover, there is evidence that the fate of superconductivity and CDWs are intertwined in La-based cuprates with stripes.

Significance

The origin of high-temperature superconductivity remains unknown. Over the past two decades, spatial oscillations of the electronic density known as charge-density waves (CDWs) have been found to coexist with high-temperature superconductivity in most prominent cuprate superconductors. The debate on whether CDWs help or hinder high-temperature superconductivity in cuprates is still ongoing. In principle, disorder at the atomic scale should strongly suppress both high-temperature superconductivity and CDWs. In this work, however, we find that disorder created by irradiation increases the superconducting critical temperature by 50% while suppressing the CDW order, showing that CDWs strongly hinder bulk superconductivity. We provide indications that this increase occurs because the CDWs could be part of a pair-density wave frustrating the superconducting coupling between atomic planes.

Author contributions: M.L. and V.M. designed research; M.L., J.P.C.R., H.C., M.P.S., C.O., P.R., A.K., G.D.G., J.M.T., W.-K.K., Z.I., and U.W. performed research; C.O., P.R., G.D.G., and J.M.T. contributed new reagents/analytic tools; M.L., V.M., J.P.C.R., H.C., M.P.S., J.M.T., W.-K.K., Z.I., and U.W. analyzed data; V.M. gave conceptual advice; and M.L., V.M., P.R., J.M.T., W.-K.K., Z.I., and U.W. wrote the paper.

The authors declare no conflict of interest.

This article is a PNAS Direct Submission.

[1]To whom correspondence may be addressed. Email: maxime@lanl.gov or welp@anl.gov.

[2]Present address: Materials Physics and Applications Division, Condensed Matter and Magnet Science Group, Los Alamos National Laboratory, Los Alamos, NM 87545.

[3]Present addresses: Computational Sciences and Engineering Division and Center for Nanophase Materials Sciences, Oak Ridge National Laboratory, Oak Ridge, TN 37831.

[4]Present address: Department of Physics and Astronomy, Hofstra University, Hempstead, NY 11549.

This article contains supporting information online at www.pnas.org/lookup/suppl/doi:10.1073/pnas.1817134116/-/DCSupplemental.

Published online May 13, 2019.

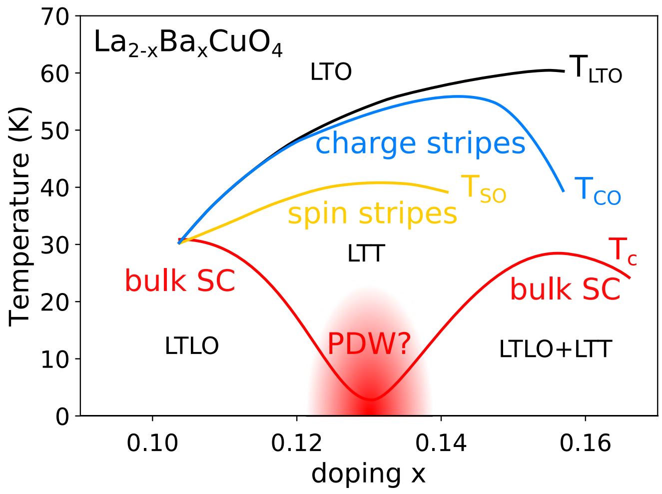

Fig. 1. Schematic phase diagram of $La_{2-x}Ba_xCuO_4$. A marked suppression of the superconducting critical temperature (T_c) occurs at ∼1/8 doping. At this doping level, charge and spin stripe order is the most pronounced. It has been proposed that the stripe order is accompanied by a PDW state. Structural phases: low-temperature orthorhombic (LTO), low-temperature tetragonal (LTT), and low-temperature less-orthorhombic (LTLO). Data are adapted from ref. 6.

Angle-resolved photo-emission spectroscopy data are consistent with a phase-incoherent d-wave superconductor whose Cooper pairs form spin-charge-ordered structures instead of becoming superconducting (35). Extremely small in-plane resistance was also found in the stripe phase above the superconducting T_c (36, 37). Further evidence for "in-plane" superconductivity in the normal-state striped phase of LBCO (above the bulk superconducting T_c) was found in the nonlinear optical response, with clear signatures of superconducting tunneling above T_c and up to the CDW transition temperature (9). A recovery of the interlayer Josephson coupling, marked by a rapid and transient blue shift of the Josephson plasmon resonance, was also observed when the stripe order was melted by near-infrared femtosecond laser pulses (38). It was also shown that the spin-stripe ordering temperature is suppressed in the same manner as the superconducting transition temperature when doping with Zn (10), which strongly suggests that the existence of stripes requires intertwining with superconducting pairing correlations. Nonmagnetic Zn impurities are indeed known to suppress T_c in cuprates (39, 40).

A leading hypothesis to explain these anomalies is the so-called PDW state: a condensate of Cooper pairs (electron–electron pairs) with a finite center of mass momentum, giving rise to real-space modulations with no uniform component (25, 37, 41, 42). In a recent scanning tunneling microscopy experiment, detection of PDW order in vortex cores has further supported the idea of PDWs' relevance for cuprates (43). Because stripes are oriented perpendicular to one another in adjacent planes in cuprates, a PDW would have no first-order Josephson coupling between adjacent planes, in agreement with the nonlinear optical response (9, 38). The PDWs' inherent frustration of the Josephson coupling would also yield zero in-plane resistance, but no bulk Meissner effect and zero critical current (41), in agreement with transport and magnetization studies (36, 37). As CDWs and PDWs are modulated in real space, they should have a strong sensitivity to disorder (41).

In this work, we prove that CDWs and bulk superconductivity are strongly competing in LBCO close to 1/8 doping. In this cuprate, we observed a striking increase of T_c and suppression of the CDWs after increasing the disorder via irradiation, in sharp contrast with the expected behavior of a d-wave superconductor. Beyond the competing CDW scenario, our results would also have a natural explanation in the PDW scenario, in terms of a restored Josephson coupling. This would imply that the PDWs are impeding the bulk d-wave superconductivity in LBCO. More generally, our results establish irradiation-induced disorder as a particularly relevant tuning parameter to study the many families of superconductors that have coexisting density waves and other spatially modulated orders.

Results

In Fig. 2, we report magnetization measurements showing the expulsion of the magnetic field (Meissner effect) in a 75-µm-thick, 1/8-doped LBCO single crystal which was repeatedly irradiated with 5-MeV protons. The bulk T_c, defined as the midpoint of the transition to a complete Meissner effect, was enhanced by up to 50% as the cumulative irradiation dose increased. This behavior was consistently observed across several samples of LBCO, as reported in Fig. 2, *Upper*. Notice also how up to 10×10^{16} p/cm^2, the magnetization curves stay sharp and parallel. The curves simply shift uniformly to higher and higher temperature after irradiation, indicating that the superconducting properties stay uniform. For the two highest irradiation doses (14.1 and 18.1×10^{16} p/cm^2), the curves finally start to broaden and shift back to lower temperature; such high doses are comparable to those known to degrade cuprate superconductors properties (44).

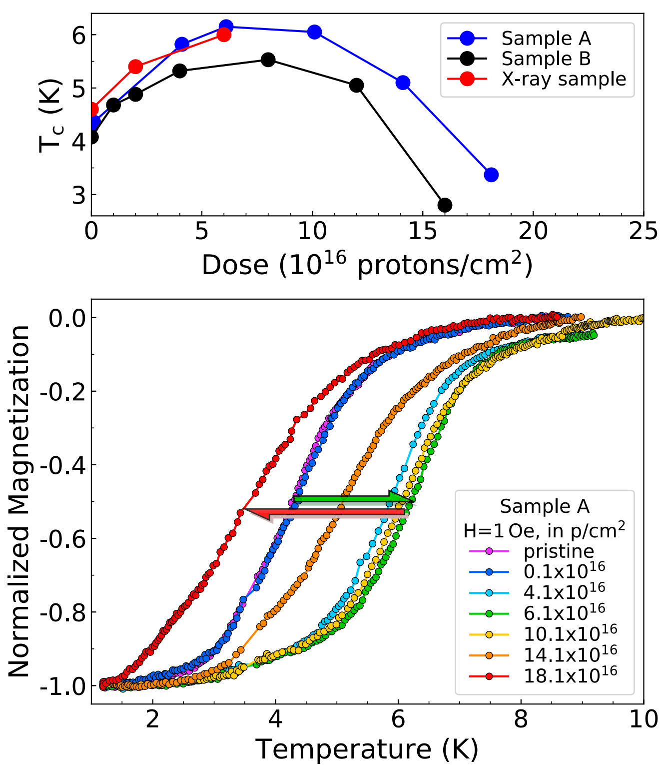

Fig. 2. Irradiation enhances superconductivity in $La_{1.875}Ba_{0.125}CuO_4$. (*Upper*) Evolution of the superconducting transition temperature T_c (defined as a 50% reduction in magnetization to a complete Meissner effect) of several samples of $La_{1.875}Ba_{0.125}CuO_4$, as a function of irradiation dose. (*Lower*) Normalized magnetization of $La_{1.875}Ba_{0.125}CuO_4$ showing the temperature evolution of the Meissner effect as a function of 5-MeV proton-irradiation dose. A clear increase of T_c is observed, in contrast with the expected behavior of a normal d-wave superconductor. The transition temperature, which starts out at 4.28 K, peaks at 6.15 K after irradiation to 6.1×10^{16} p/cm^2, and then falls back to 3.37 K after the last irradiation. The T_c curves stay sharp after the first four irradiations, indicative of uniform superconducting properties and uniform irradiation damage.

As mentioned in the introduction and Fig. 1, LBCO has charge and spin-stripe orders and undergoes a series of separate transitions as a function of temperature (37): The resistivity of the *ab* plane drops below $T_{SDW} = 42\ K$ and becomes immeasurably small ($< 10^{-4}$ mΩ·cm) at $T_{KT} \approx 16$ K. In between, the dependence is qualitatively of the Berezinskii–Kosterlitz–Thouless form, suggesting superconducting fluctuations restricted to individual copper-oxide planes. The resistivity of the *c* axis also vanishes, but only below $T_{3D} \approx 10$ K, so that, within experimental errors, the anisotropy of the resistivity is infinite between T_{3D} and T_{KT}. Finally, the Meissner effect occurs below 4 K, which has been considered as the true T_c (36, 37). We performed a series of complementary measurements which agreed with the magnetization measurements and revealed a richer picture.

In Fig. 3, we show the frequency shift in tunnel diode oscillator (TDO) measurements, which is proportional to the length over which the external magnetic field is screened (45, 46). In the normal state, this is the skin depth (δ), and in the superconducting state, it is the magnetic penetration depth (λ). The small ($\approx 5\,\mu$T) magnetic field oscillating near 14 MHz mostly probed the in-plane λ_{ab} when applied along the *c* axis (Fig. 3, *Upper*). The frequency started to decrease at <18 K, where the in-plane resistivity was reported to tend toward zero (36) and in agreement with previous studies (37) which provide evidence for the onset of in-plane superconductivity below $T_{KT} \approx$ 16 K. Then, a faster decrease occurred at <5 K where the Meissner effect was observed in magnetization measurements. Strikingly, only the part <5 K shifted toward higher temperature after irradiation, and the midpoint of this transition shifted from 4.5 to 5.0 K for 2×10^{16} p/cm^2, in excellent agreement with the magnetization measurements of Fig. 2. When the field was applied in-plane, both λ_{ab} and λ_c were probed. Again, the frequency started to decrease at <18 K and decreased faster at <5 K, but there was a global shift toward higher temperature after irradiation, which is suggestive of enhanced *c*-axis superconducting Josephson coupling, as we will discuss later.

We also measured the temperature dependence of the in-plane resistivity of another LBCO crystal from the same batch after successive irradiations (Fig. 4). The resistivity curves globally shift to higher values as the irradiation dose is increased, as expected from increased disorder. The residual resistivities at zero temperature by extrapolation of the high-temperature linear behavior are 2.25, 2.41, and 3.15 mΩ·cm (which would be 34, 37, and 48 kΩ per CuO_2 plane, but this includes a significant *c*-axis contribution; see below). For LSCO $x = 0.10$, adding 2% Zn caused the in-plane resistivity to more than double (39); thus, the relative change in resistivity for LBCO is comparable to somewhat less than 1% Zn doping. At low temperature, the resistivity of our sample dropped below the sensitivity of our instruments ($10^{-7}\,\Omega$·cm) at <8 K for all curves, a few kelvins above the Meissner effect we observed at 4 K. The value of 8 K was closer to the 10 K temperature reported for the *c*-axis transition to zero resistance (36, 37). We attribute this fact and the shape of the resistivity (compared with ref. 36) to our sample being slightly misaligned from the in-plane direction (by at most 3.5°, from the absolute value of the resistivity) and the extremely large anisotropy of the resistivity ρ_c/ρ_{ab} at low temperature (36) (2×10^3 to $> 10^5$). But this did not prevent us from observing the superconducting transition and, most importantly, the structural and CDW transitions visible in the resistivity of both axes. In fact, in the derivative of the resistivity, we observed a dip at 55.3 K, which matches well with the known orthorhombic-to-tetragonal structural transition. This transition temperature did not seem to change after the first irradiation and was smoothed out after the second. A second dip in the derivative, at a temperature immediately below the structural transition, appeared to coincide well with the CDW transition. This transition seemed to shift from 52.5 K to 50 K after the first irradiation and may reach 35 K after the second. Finally, the large maximum in resistivity usually associated with the spin-stripe order clearly shifted toward lower temperature after irradiation.

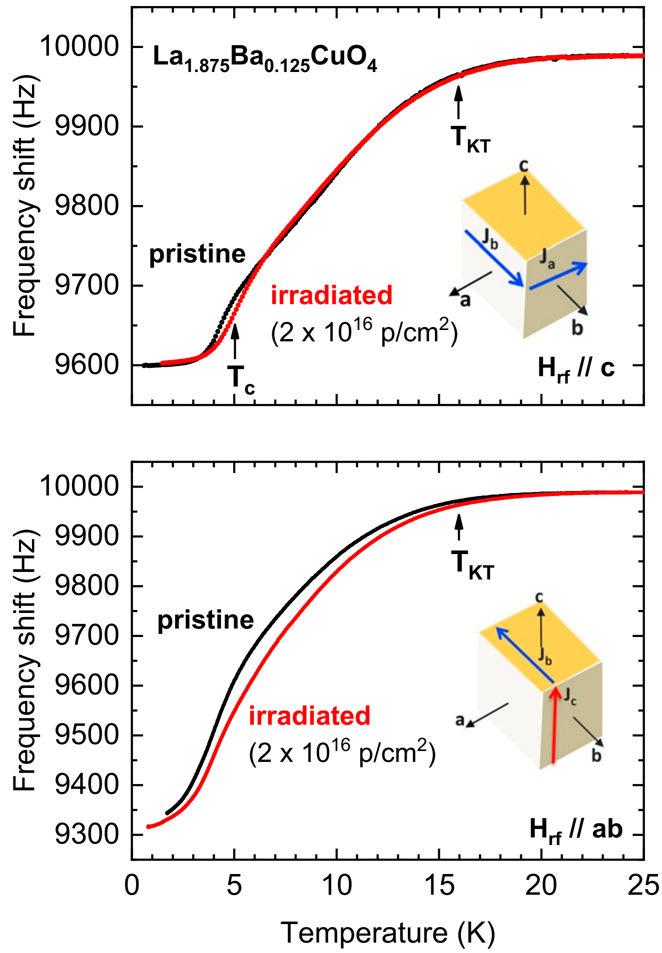

Fig. 3. TDO measurements show enhanced superconductivity after irradiation. The frequency shift of the oscillator is proportional to the superconducting magnetic penetration depth (λ). (*Upper*) When parallel to the *c* axis (*Inset*), the small (microtesla) oscillating magnetic field probes mostly the in-plane λ_{ab}. Below 5 K, the small shift toward higher temperature after irradiation is in agreement with the change in Meissner effect reported in Fig. 2. (*Lower*) When the field is aligned in-plane, it probes both λ_{ab} and λ_c. In this case, we observe a global shift toward higher temperature, which is suggestive of enhanced *c*-axis Josephson coupling. The Kosterlitz–Thouless (KT) temperature reported in ref. 37 is also indicated by an arrow.

To investigate the effect of irradiation on the CDW, we performed X-ray diffraction measurements. Fig. 5 shows the temperature dependence of the integrated intensity of the CDW peak at (0.233, 0, 8.5) after several irradiations. In between irradiations, we also checked that the sample showed a similar T_c increase (compare Fig. 2). While the onset of the CDW phase does not appear to change within our temperature resolution, the CDW peak intensity clearly grew more slowly after irradiation. The midpoint of this evolution shifts to lower temperature at a rate of $1.0\,\mathrm{K}/10^{16}\,\mathrm{p/cm^2}$. The precise onset of the CDW order is challenging to determine because of the finite correlation length, which is reduced by irradiation; in addition, dynamic CDW correlations have been reported above the CDW

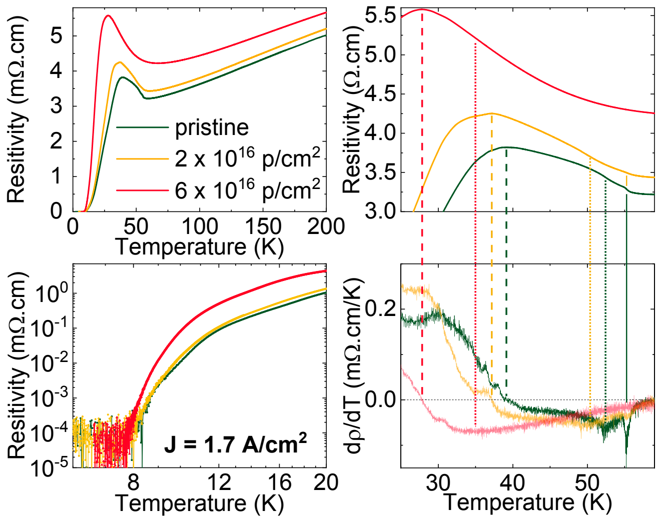

Fig. 4. Resistivity suggests suppressed charge order after irradiation. (*Upper Left*) Temperature dependence of the in-plane resistivity of LBCO (with a small *c*-axis component; text) as a function of irradiation dose. Increased disorder yields the expected global upward shift. (*Lower Left*) Log–log plot of the resistivity near the superconducting transition. As reported in ref. 37, the resistivity drops rapidly a few kelvins above the Meissner effect at 4 K. The resistivity gets steeper after irradiation, suggesting a possible crossing below the sensitivity of our instruments ($10^{-7}\ \Omega{\cdot}$cm). (*Right*) Resistivity and its derivative as a function of temperature around the structural and CDW transitions. A solid line indicates the structural transition at 55.3 K, dotted lines indicate the inflection point at a temperature immediately below which seems to match the CDW transition, and dashed lines indicate the maximum resistivity.

transition temperature (8). After irradiation, the CDW peak also broadened from 0.017 to 0.02 a^*, so that the in-plane long-range coherence of the CDW, defined as 1/width, was reduced from 223 to 189 Å.

Discussion

Irradiation of superconductors typically leads to a decrease of T_c and an increase of the resistivity (40, 47, 48). This phenomenology is broadly consistent with expectations based on irradiation-induced pair-breaking scattering (49–51). However, the increase of T_c reported here cannot be accounted for in these models. Recently, it has been shown (52) that in a very inhomogeneous spin-fluctuation-mediated unconventional superconductor, spatial averaging over the inhomogeneous gap can, under certain conditions, result in an increase of T_c. We believe, though, that our samples do not fall into the regime considered in this work. The question then arises whether our results are caused by another extrinsic effect, such as an irradiation-induced change in doping level. Irradiation does cause atomic displacements which disrupt the local electronic states and which could, in principle, lead to additional charge transfer and an increase or decrease of T_c. Cooling the samples during irradiation to -10°C and the use of beam currents of <100 nA (44) prevent beam-induced sample heating and an associated potential loss of oxygen from the sample. Furthermore, extensive work on the effect of irradiation in cuprate superconductors with various particles (53–55) has shown that the Hall coefficient at low temperature does not change upon irradiation, even to remarkably high doses. Thus, to the extent that the Hall number in these materials is a measure of their charge count, the doping level is independent of irradiation. In addition, our samples afford an intrinsic gauge of the doping level since the incommensurate CDW vector is doping-dependent (56). As shown in SI Appendix, the CDW wavevector does not change within the resolution of our measurements: (0.229, 0, 0.5) ± 0.0014 in the pristine sample and (0.231, 0, 0.5) ± 0.0014 in the irradiated sample, respectively, implying that any change in doping is negligible. Hence, we conclude that our observations are not extrinsic in origin, but a reflection of the response of the superconducting order and of the charge order to irradiation-induced defects. Then, in a picture of straight competition between superconducting and charge order, an increase of T_c naturally arises if the detrimental effect of irradiation-induced disorder is stronger on the charge order than it is on superconductivity (57–60). Indeed, it has been shown that disorder either due to irradiation (refs. 26 and 61, p. 52) or substitution (62) strongly suppresses the CDW state, either due to pair-breaking (63) or real-space phase fluctuations (64, 65). Hence, we conclude that the charge-stripe order is strongly competing with bulk superconductivity in $La_{1.875}Ba_{0.125}CuO_4$.

Beyond this competition scenario, the TDO data also provide indications for a possible PDW scenario. TDO data indeed show enhanced magnetic screening below 18 K after irradiation, when the field is in-plane (Fig. 3, *Lower*), which cannot be explained by the standard effects of disorder. In the normal state, irradiation should increase resistivity and the skin depth, and in the superconducting state, disorder should also increase λ. Therefore, our results points to a reduced λ_c and enhanced *c*-axis Josephson coupling between layers as the most likely cause for

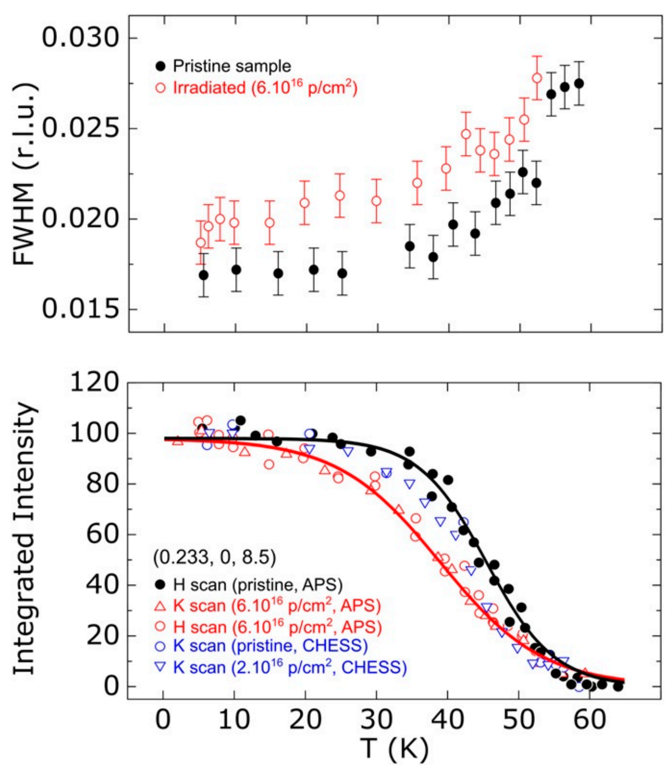

Fig. 5. Irradiation suppresses the CDWs in $La_{1.875}Ba_{0.125}CuO_4$. (*Upper*) Temperature dependence of the in-plane full-width at half-maximum (FWHM) of the CDW peak at (0.233; 0; 8.5) and 8.900 keV, before and after irradiation in the same sample. r.l.u., reciprocal lattice units. (*Lower*) Temperature dependence of the integrated intensity of the CDW peak at (0.233; 0; 8.5) for both *h*-d and k-scan and for both 8.9 keV [Advanced Photon Source (APS)] and 27 keV [Cornell High Energy Synchrotron Source (CHESS)]. The growth of the order parameter of the CDW state is systematically suppressed by irradiation, but no significant shift of the onset of the CDWs is observed within our temperature resolution.

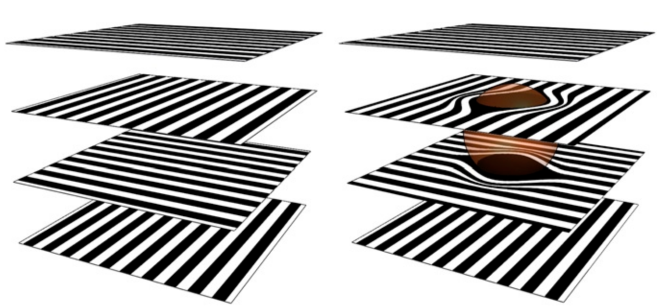

Fig. 6. Disorder-mediated 3D coupling reestablishes Josephson coupling. (*Left*) In an ideal PDW, orthogonal charge-spin stripes in adjacent layers prevent Josephson coupling between layers. (*Right*) In the presence of disorder, distorted stripes around defects are no more orthogonal, which reestablishes Josephson coupling between layers.

this enhanced magnetic screening (λ_{ab} only changes below 5 K, as shown in Fig. 3, *Upper*).

It has been proposed that the frustration of the interlayer Josephson tunneling and corresponding suppression of the bulk T_c is the consequence of a pair-density-wave order associated with the stripe order in the CuO_2 planes (37) and that this coupling can be recovered upon melting the stripe order with femtosecond laser pulses (9, 38). With perfect PDW order, the spatially alternating sign of the pair wave function leads to a cancellation of the interlayer Josephson coupling. Therefore, any perturbation of the perfect stripe structure—for example, due to irradiation-induced defects as depicted in Fig. 6—would cause an increase in the Josephson coupling between layers and a rise in T_c. Although the initial evidence for the PDW order in LBCO has been indirect, new experiments are providing direct evidence in support of the occurrence of PDW superconductivity in cuprates (43, 66). Nevertheless, the PDW scenario and its alternatives are still an actively researched open question.

Finally, we point out that competition between superconductivity and CDW or other spatially modulated order is ubiquitous in many families of superconductors. For instance, in the Fe-based superconductors, an SDW state appears to compete with superconductivity (57, 58), and the underlying magnetism is thought to be a key ingredient for superconductivity. Similarly, in heavy Fermion compounds such as $CeCoIn_5$, the interaction between SDW and d-wave superconductivity is still being actively investigated (71). This topic is also a staple of the dichalcogenides superconductors, in which CDW were first discovered. The case for competition is relatively well established in 2H-TaS_2 and -$TaSe_2$ (26). Conversely, there are claims of CDW-enhanced excitonic superconductivity in 1T-$TiSe_2$ (72). As for 2H-$NbSe_2$, the situation is complex, as the two states are only marginally related with potentially both synergy and competition (68, 73). Coexisting density waves and superconductivity are also found in the organic superconductors such as $(TMTSF)_2PF_6$ (74). To confirm this concept of irradiation as a probe of CDW-superconductivity competition, we performed a similar study on crystals of $Lu_5Ir_4Si_{10}$, which is an s-wave superconductor below 4 K with a well-characterized quasi-1D CDW below 77 K (27–29, 75, 76). The superconductivity and CDW are well known to compete in this compound (27, 28). As can be seen in Fig. 7, the increase of T_c and reduction of T_{CDW} are strikingly analogous to LBCO. For completeness, we summarized all irradiation studies on CDW-superconductivity competition in Fig. 7. The clarity of the results, but scarcity of data, clearly demonstrates the untapped potential of this technique. Interestingly, beyond its fundamental aspect, a potential application of such increased T_c via irradiation beams could be the direct write of superconducting circuits and Josephson junctions by focused irradiation beams (77), which also present the advantage that the superconducting circuits would have much irradiation-induced disorder and thus good vortex-pinning properties.

Conclusion

In summary, we observed a striking increase of T_c in $La_{1.875}Ba_{0.125}CuO_4$ after irradiation, in contrast with the behavior expected of a d-wave superconductor. This increase in T_c was accompanied by a suppression of the CDW, thus evidencing the strong competition between CDW and bulk superconductivity in

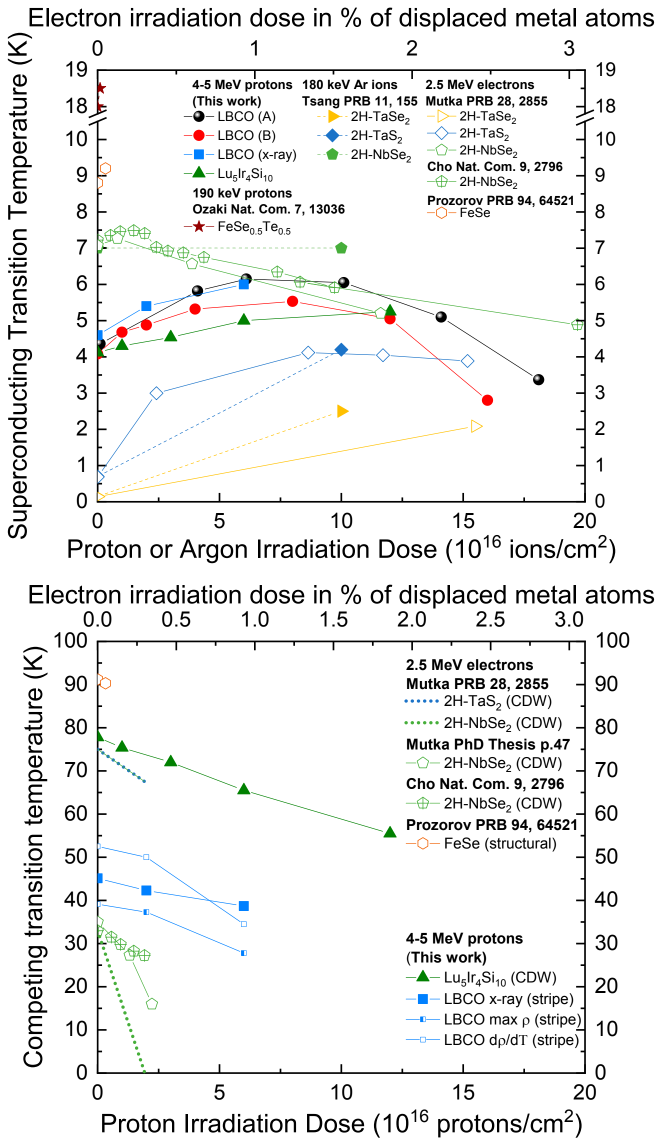

Fig. 7. Irradiation-induced disorder increases T_c and suppresses coexisting orders in several superconductors. (*Upper*) All known examples of T_c increase after irradiation, to the best of our knowledge. In this work, we report a striking increase of T_c after proton irradiation in the d-wave cuprate superconductor $La_{1.875}Ba_{0.125}CuO_4$ and a similar, albeit expected, T_c increase in $Lu_5Ir_4Si_{10}$, an s-wave superconductor with a strong 1D CDW. Increases of T_c have been reported in s-wave dichalcogenides by using both argon (67) and electron irradiation (26, 61, 68), and possible hints can be found in iron-based superconductors (69, 70). (*Lower*) In parallel to the increase of T_c, a coexisting order was found to be suppressed in some of these compounds. Dotted lines are reported initial trends. Cho Nat. Com., ref. 68; Mutka PhD Thesis, ref. 61; Mutka PRB, ref. 26; Ozaki Nat. Com., ref. 69; Prozorov PRB, ref. 70; Tsang PRB, ref. 67.

PHYSICS

$La_{1.875}Ba_{0.125}CuO_4$. TDO data also point to the restoration of interlayer Josephson coupling frustrated by charge-spin stripes, which would be compatible with a PDW state competing with a uniform d-wave component.

Materials and Methods

$La_{1.875}Ba_{0.125}CuO_4$ Samples. The samples of LBCO were grown by G.D.G. LBCO has a tetragonal crystal structure with space group I4/mmm and lattice parameters *a* = 3.788 and *c* = 13.23 Å(78). LBCO samples, cut and polished down to 75-μm thickness along the *c* axis, were repeatedly irradiated with 5-MeV protons by using the tandem van de Graaff accelerator at Western Michigan University. The stopping and range of ions in matter (SRIM) calculations (79) predicted a penetration depth of 103 μm at this energy, thus ensuring uniform irradiation damage and negligible proton implantation. We used typical beam currents of 500 nA spread over 1 cm^2. The irradiation dose was measured by integrating the total current from the irradiation chamber to avoid double counting. The sample was actively cooled to about -10°C during irradiation to avoid heat damage. Upstream slits defined a beam spot size of maximum 4.7-mm diameter at the entrance of the irradiation chamber. A subsequent 1-μm-thick gold foil and collimator pair ensured the homogeneity of the incident beam.

Superconducting Quantum Interference Device. The critical temperature of LBCO was measured by using the standard zero-field cooled procedure in a custom superconducting quantum interference device magnetometer in a field of 1 oersted applied by a copper coil.

Resistivity. Resistivity measurements were performed in a custom ^{4}He cryostat on a 1-mm × 160-μm × 75-μm crystal, by using a Keithley 2182 voltmeter and a Keithley 6221 current source with a current of 200 μA.

TDO. Magnetic penetration depth measurements were performed by using a TDO operating at 14 MHz in a ^{3}He cryostat.

X-Ray. X-ray diffraction studies were carried out on 6-ID-B,C at the APS. Data were collected in reflection geometry by using 8.9-keV photons. X-ray diffraction studies were carried on A2 at CHESS. Data were collected in transmission geometry by using 27-keV photons.

$Lu_5Ir_4Si_{10}$ Samples. $Lu_5Ir_4Si_{10}$ is a quasi-1D material with a tetragonal P4/mbm space group symmetry and lattice parameters *a* = 12.484 (1) and *c* = 4.190 (2) Å (80). The samples of $Lu_5Ir_4Si_{10}$ were grown at the Néel Institute by C.O. They grew spontaneously in needle form and have already been characterized (29, 80). These needles are high-quality single crystals and naturally grow along the *c* axis, which is also the axis of the CDW. One sample with as-grown dimensions of 10 μm × 65 μm × 500 μm (a × b × c) was repeatedly irradiated with 4-MeV protons at Western Michigan University, by using the same irradiation procedure as LBCO. At this energy, the projected range of protons is 67 μm, according to SRIM calculations (79), ensuring uniform irradiation damage. Resistivity measurements were taken by using a Keithley 2182 voltmeter and a Keithley 6221 current source, in a custom ^{4}He cryostat.

ACKNOWLEDGMENTS. M.L. and U.W. thank Y.-L. Wang for the 3D-coupling schematic. The experimental study at Argonne National Laboratory was supported by the US Department of Energy (DOE), Office of Science, Materials Sciences and Engineering Division. V.M. was supported by the Center for Emergent Superconductivity, an Energy Frontier Research Center, funded by the US DOE, Office of Science, Office of Basic Energy Sciences. The work at Brookhaven National Laboratory was supported by the US DOE, Office of Basic Energy Sciences, Division of Materials Sciences and Engineering, under Contract DE-SC0012704. Proton irradiation was performed at Western Michigan University. This research used resources of the APS, a US DOE Office of Science User Facility operated for the DOE Office of Science by Argonne National Laboratory under Contract DE-AC02-06CH11357. High-energy transmission X-ray data were collected on beamline A2 at CHESS, which is supported by the National Science Foundation (NSF) and the National Institutes of Health/National Institute of General Medical Sciences under NSF Award DMR-1332208.

1. Grüner G (2000) *Density Waves in Solids*, Frontiers in Physics (Westview Press, Boulder, CO), vol 89.
2. Tranquada JM, Sternlieb BJ, Axe JD, Nakamura Y, Uchida S (1995) Evidence for stripe correlations of spins and holes in copper oxide superconductors. *Nature* 375:561–563.
3. Tranquada JM, et al. (1997) Coexistence of, and competition between, superconductivity and charge-stripe order in $La_{1.6-x}Nd_{0.4}Sr_xCuO_4$. *Phys Rev Lett* 78:338–341.
4. Fujita M, Goka H, Yamada K, Matsuda M (2002) Competition between charge- and spin-density-wave order and superconductivity in $La_{1.875}Ba_{0.125-x}Sr_xCuO_4$. *Phys Rev Lett* 88:167008.
5. Kim Y-J, Gu GD, Gog T, Casa D (2008) X-ray scattering study of charge density waves in $La_{2-x}Ba_xCuO_4$. *Phys Rev B* 77:064520.
6. Hücker M, et al. (2011) Stripe order in superconducting $La_{2-x}Ba_xCuO_4$ ($0.095 < x < 0.155$). *Phys Rev B* 83:104506.
7. Jie Q, Jung Han S, Dimitrov I, Tranquada JM, Li Q (2012) Transport properties of stripe-ordered high T_c cuprates. *Phys C Supercond Appl* 481:46–54.
8. Miao H, et al. (2017) High-temperature charge density wave correlations in $La_{1.875}Ba_{0.125}CuO_4$ without spin-charge locking. *Proc Natl Acad Sci USA* 114:12430–12435.
9. Rajasekaran S, et al. (2018) Probing optically silent superfluid stripes in cuprates. *Science* 359:575–579.
10. Guguchia Z, et al. (2017) Complementary response of static spin-stripe order and superconductivity to nonmagnetic impurities in cuprates. *Phys Rev Lett* 119:087002.
11. George Bednorz J, Alex Müller K (1986) Possible high T_c superconductivity in the Ba-La-Cu-O system. *Z Phys B Condens Matter* 64:189–193.
12. Fujita M, Goka H, Yamada K, Tranquada J, Regnault L (2004) Stripe order, depinning, and fluctuations in $La_{1.875}Ba_{0.125}CuO_4$ and $La_{1.875}Ba_{0.075}Sr_{0.050}CuO_4$. *Phys Rev B* 70:104517.
13. Wu T, et al. (2011) Magnetic-field-induced charge-stripe order in the high-temperature superconductor $YBa_2Cu_3O_y$. *Nature* 477:191–194.
14. Wu T, et al. (2013) Emergence of charge order from the vortex state of a high-temperature superconductor. *Nat Commun* 4:2113.
15. Wu T, et al. (2015) Incipient charge order observed by NMR in the normal state of $YBa_2Cu_3O_y$. *Nat Commun* 6:6438.
16. Le Tacon M, et al. (2013) Inelastic X-ray scattering in $YBa_2Cu_3O_{6.6}$ reveals giant phonon anomalies and elastic central peak due to charge-density-wave formation. *Nat Phys* 10:52–58.
17. Chang J, et al. (2012) Direct observation of competition between superconductivity and charge density wave order in $YBa_2Cu_3O_{6.67}$. *Nat Phys* 8:871–876.
18. Gerber S, et al. (2015) Three-dimensional charge density wave order in $YBa_2Cu_3O_{6.67}$ at high magnetic fields. *Science* 350:949–952.
19. Jang H, et al. (2016) Ideal charge-density-wave order in the high-field state of superconducting YBCO. *Proc Natl Acad Sci USA* 113:14645–14650.
20. da Silva Neto EH, et al. (2014) Ubiquitous interplay between charge ordering and high-temperature superconductivity in cuprates. *Science* 343:393–396.
21. Tabis W, et al. (2014) Charge order and its connection with Fermi-liquid charge transport in a pristine high-T_c cuprate. *Nat Commun* 5:5875.
22. da Silva Neto EH, et al. (2015) Charge ordering in the electron-doped superconductor $Nd_{2-x}Ce_xCuO_4$. *Science* 347:282–285.
23. Kacmarcik J, et al. (2018) Unusual interplay between superconductivity and field-induced charge order in $YBa_2Cu_3O_y$. arXiv:1805.06853v1. Preprint, posted May 17, 2018.
24. Yu F, et al. (2016) Magnetic phase diagram of underdoped $YBa_2Cu_3O_y$ inferred from torque magnetization and thermal conductivity. *Proc Natl Acad Sci USA* 113:12667–12672.
25. Fradkin E, Kivelson SA, Tranquada JM (2015) Colloquium: Theory of intertwined orders in high temperature superconductors. *Rev Mod Phys* 87:457–482.
26. Mutka H (1983) Superconductivity in irradiated charge-density-wave compounds 2H-$NbSe_2$, 2H-TaS_2, and 2H-$TaSe_2$. *Phys Rev B* 28:2855–2858.
27. Shelton RN, et al. (1986) Electronic phase transition and partially gapped Fermi surface in superconducting $Lu_5Ir_4Si_{10}$. *Phys Rev B* 34:4590–4594.
28. Singh Y, Nirmala R, Ramakrishnan S, Malik SK (2005) Competition between superconductivity and charge-density-wave ordering in the $Lu_5Ir_4(Si_{1-x}Ge_x)_{10}$ alloy system. *Phys Rev B* 72:045106.
29. Leroux M, Rodière P, Opagiste C (2013) Charge density wave and superconducting properties in single crystals of $Lu_5Ir_4Si_{10}$. *J Supercond Novel Magn* 26:1669–1672.
30. Ramshaw BJ, et al. (2015) Quasiparticle mass enhancement approaching optimal doping in a high-T_c superconductor. *Science* 348:317–320.
31. Cava RJ, et al. (1988) Structural anomalies at the disappearance of superconductivity in $Ba_2YCu_3O_{7-\delta}$: Evidence for charge transfer from chains to planes. *Phys C Supercond* 156:523–527.
32. Moodenbaugh AR, Xu Y, Suenaga M, Folkerts TJ, Shelton RN (1988) Superconducting properties of $La_{2-x}Ba_xCuO_4$. *Phys Rev B* 38:4596–4600.
33. Kim J, Kagedan A, Gu GD, Nelson CS, Kim Y-J (2008) Magnetic field dependence of charge stripe order in $La_{2-x}Ba_xCuO_4$ ($x \approx 1/8$). *Phys Rev B* 77:180513.
34. Ido M, et al. (1996) Pressure effect on anomalous suppression of T_c around x=1/8 in $La_{2-x}Ba_xCuO_4$ and $La_{1.8-x}Nd_{0.2}Ba_xCuO_4$. *J Low Temp Phys* 105:311–316.
35. Valla T, Fedorov AV, Lee J, Davis JC, Gu GD (2006) The ground state of the pseudogap in cuprate superconductors. *Science* 314:1914–1916.
36. Li Q, Hücker M, Gu GD, Tsvelik AM, Tranquada JM (2007) Two-dimensional superconducting fluctuations in stripe-ordered $La_{1.875}Ba_{0.125}CuO_4$. *Phys Rev Lett* 99:067001.
37. Berg E, et al. (2007) Dynamical layer decoupling in a stripe-ordered high-T_c superconductor. *Phys Rev Lett* 99:127003.
38. Khanna V, et al. (2016) Restoring interlayer Josephson coupling in $La_{1.885}Ba_{0.115}CuO_4$ by charge transfer melting of stripe order. *Phys Rev B* 93:224522.
39. Fukuzumi Y, Mizuhashi K, Takenaka K, Uchida S (1996) Universal superconductor-insulator transition and T_c depression in Zn-substituted high-T_c cuprates in the underdoped regime. *Phys Rev Lett* 76:684–687.

40. Alloul H, Bobroff J, Gabay M, Hirschfeld PJ (2009) Defects in correlated metals and superconductors. *Rev Mod Phys* 81:45–108.
41. Berg E, Fradkin E, Kivelson SA, Tranquada JM (1996) Striped superconductors: How spin, charge and superconducting orders intertwine in the cuprates. *New J Phys* 11:115004.
42. Tranquada JM, et al. (2008) Evidence for unusual superconducting correlations coexisting with stripe order in $La_{1.875}Ba_{0.125}CuO_4$. *Phys Rev B* 78:174529.
43. Edkins SD, et al. (2018) Magnetic-field induced pair density wave state in the cuprate vortex halo. arXiv:1802.04673v2. Preprint, posted February 14, 2018.
44. Jia Y, et al. (2013) Doubling the critical current density of high temperature superconducting coated conductors through proton irradiation. *Appl Phys Lett* 103:122601.
45. Smylie MP, et al. (2016) Evidence of nodes in the order parameter of the superconducting doped topological insulator $Nb_xBi_2Se_3$ via penetration depth measurements. *Phys Rev B* 94:180510.
46. Smylie MP, et al. (2016) Effect of proton irradiation on superconductivity in optimally doped $BaFe_2(As_{1-x}P_x)_2$ single crystals. *Phys Rev B* 93:115119.
47. Rullier-Albenque F, Alloul H, Tourbot R (2003) Influence of pair breaking and phase fluctuations on disordered high T_c cuprate superconductors. *Phys Rev Lett* 91:047001.
48. Rullier-Albenque F, et al. (2000) Universal T_c depression by irradiation defects in underdoped and overdoped cuprates? *Europhys Lett* 50:81–87.
49. Anderson PW (1959) Theory of dirty superconductors. *J Phys Chem Sol* 11:26–30.
50. Abrikosov AA, Gor'kov LP (1961) Contribution to the theory of superconducting alloys with paramagnetic impurities. *Sov Phys JETP* 12:1243.
51. Openov LA (1998) Critical temperature of an anisotropic superconductor containing both nonmagnetic and magnetic impurities. *Phys Rev B* 58:9468–9478.
52. Rømer AT, Hirschfeld PJ, Andersen BM (2018) Raising the critical temperature by disorder in unconventional superconductors mediated by spin fluctuations. *Phys Rev Lett* 121:027002.
53. Legris A, Rullier-Albenque F, Radeva E, Lejay P (1993) Effects of electron irradiation on $YBa_2Cu_3O_{7-\delta}$ superconductor. *J Phys France* 3:1605–1615.
54. Valles JM, et al. (1989) Ion-beam-induced metal-insulator transition in $YBa_2Cu_3O_{7-\delta}$: A mobility edge. *Phys Rev B* 39:11599–11602.
55. Goshchitskii BN, Davydov SA, Karkin AE, Mirmelstein AV (1989) Hall effect in disordered ceramic high-T_c $YBa_2Cu_3O_7$. *Physica C: Superconductivity its Appl* 162-164:997–998.
56. Hücker M, et al. (2014) Competing charge, spin, and superconducting orders in underdoped $YBa_2Cu_3O_y$. *Phys Rev B* 90:054514.
57. Mishra V (2015) Effect of disorder on superconductivity in the presence of spin-density wave order. *Phys Rev B* 91:104501.
58. Fernandes RM, Vavilov MG, Chubukov AV (2012) Enhancement of T_c by disorder in underdoped iron pnictide superconductors. *Phys Rev B* 85:1–5.
59. Grest GS, Levin K, Nass MJ (1982) Impurity and fluctuation effects in charge-density-wave superconductors. *Phys Rev B* 25:4562–4569.
60. Psaltakis GC (1984) Non-magnetic impurity effects in charge-density-wave superconductors. *J Phys C Solid State Phys* 17:2145–2155.
61. Mutka H (1983) Irradiation of layered metallic dichalcogenides: Disorder in the charge density waves. PhD thesis (Université Paris-Sud, Orsay, France).
62. Chatterjee U, et al. (2015) Emergence of coherence in the charge-density wave state of 2H-$NbSe_2$. *Nat Commun* 6:6313.
63. Stiles JAR, Williams DL, Zuckermann MJ (1976) Dependence of the critical temperature for the formation of charge density waves in 2H-$NbSe_2$ upon impurity concentration. *J Phys C Solid State Phys* 9:489–493.
64. McMillan WL (1975) Landau theory of charge-density waves in transition-metal dichalcogenides. *Phys Rev B* 12:1187–1196.
65. Mutka H, Zuppiroli L, Molinié P, Bourgoin JC (1981) Charge-density waves and localization in electron-irradiated 1T-TaS_2. *Phys Rev B* 23:5030–5037.
66. Hamilton DR, Gu GD, Fradkin E, Van Harlingen DJ (2018) Signatures of pair-density wave order in phase-sensitive measurements of $La_{2-x}Ba_xCuO_4$–Nb Josephson junctions and SQUIDs. arXiv:1811.02048. Preprint, posted November 5, 2018.
67. Tsang JC, Shafer MW, Crowder BL (1975) Effect of crystal damage on superconductivity in the transition-metal layer compounds. *Phys Rev B* 11:155–162.
68. Cho K, et al. (2018) Using controlled disorder to probe the interplay between charge order and superconductivity in $NbSe_2$. *Nat Commun* 9:2796.
69. Ozaki T, et al. (2016) A route for a strong increase of critical current in nanostrained iron-based superconductors. *Nat Commun* 7:13036.
70. Teknowijoyo S, et al. (2016) Enhancement of superconducting transition temperature by pointlike disorder and anisotropic energy gap in FeSe single crystals. *Phys Rev B* 94:064521.
71. Kim DY, et al. (2016) Intertwined orders in heavy-fermion superconductor $CeCoIn_5$. *Phys Rev X* 6:041059.
72. Kusmartseva aF, Sipos B, Berger H, Forro L, Tutis E (2009) Pressure induced superconductivity in pristine 1T-$TiSe_2$. *Phys Rev Lett* 103:236401.
73. Leroux M, et al. (2015) Strong anharmonicity induces quantum melting of charge density wave in 2H-$NbSe_2$ under pressure. *Phys Rev B* 92:140303.
74. Jérome D (2004) Organic conductors: From charge density wave TTF-TCNQ to superconducting $(TMTSF)_2PF_6$. *Chem Rev* 104:5565–5592.
75. Mansart B, et al. (2012) Evidence for a Peierls phase-transition in a three-dimensional multiple charge-density waves solid. *Proc Natl Acad Sci USA* 109:5603–5608.
76. Betts JB, et al. (2002) Complete elastic tensor across the charge-density-wave transition in monocrystal $Lu_5Ir_4Si_{10}$. *Phys Rev B* 66:060106.
77. Cho EY, Zhou YW, Cho JY, Cybart SA (2018) Superconducting nano Josephson junctions patterned with a focused helium ion beam. *Appl Phys Lett* 113:022604.
78. Abbamonte P, et al. (2005) Spatially modulated 'Mottness' in $La_{2-x}Ba_xCuO_4$. *Nat Phys* 1:155–158.
79. Ziegler JF, Ziegler MD, Biersack JP (2010) SRIM—the stopping and range of ions in matter. *Nucl Instr Methods Phys Res Sect B Beam Interact Mater Atoms* 268:1818–1823.
80. Opagiste C, et al. (2010) $Lu_5Ir_4Si_{10}$ whiskers: Morphology, crystal structure, superconducting and charge density wave transition studies. *J Cryst Growth* 312:3204–3208.

PHYSICS